

PAPER • OPEN ACCESS

The effect of heat transfer on peristaltic flow of Jeffrey fluid in an inclined porous stratum

To cite this article: C K Selvi *et al* 2017 *IOP Conf. Ser.: Mater. Sci. Eng.* **263** 062027

View the [article online](#) for updates and enhancements.

Related content

- [Unsteady MHD free convection flow of rotating Jeffrey fluid embedded in a porous medium with ramped wall temperature](#)
N A Mohd Zin, I Khan and S Shafie
- [Effects of rotation and magnetic field on the nonlinear peristaltic flow of a second-order fluid in an asymmetric channel through a porous medium](#)
A. M. Abd-Alla, S. M. Abo-Dahab and H. D. El-Shahrany
- [Peristaltic flow and heat transfer of a Herschel-Bulkley fluid in an inclined non-uniform channel with wall properties](#)
G Sucharitha, K Vajravelu, S Sreenadh et al.

The effect of heat transfer on peristaltic flow of Jeffrey fluid in an inclined porous stratum

C K Selvi¹, C Haseena¹, A N S Srinivas¹ and S Sreenadh²

¹Department of Mathematics, School of Advanced Sciences, VIT University, Vellore - 632014, India

²Department of Mathematics, Sri Venkateswara University, Tirupati-517502, Andhra Pradesh, India

E-mail: anssrinivas@vit.ac.in

Abstract. This paper investigates the heat transfer effects on peristaltic transport of a Jeffrey fluid in an inclined porous stratum. The present problem is formulated under long wavelengths and low Reynolds number approximations. Regular perturbation parameter is used to solve the governing non - linear partial differential equations. The expressions for velocity, temperature, pressure gradient and volume flow rate are derived. The effects of various pertinent parameters on velocity, temperature and pressure rise are discussed graphically. The results illustrate that the influence of inclination parameter α and permeability parameter σ on flow quantities is significant. For a fixed mean flow, the pressure rise per wavelength reduces with rising values of permeability parameter where the contradictory behavior is observed for larger values of inclination parameter. The variation in velocity for different values of pertinent parameters is studied. The pressure gradient for different values of pertinent parameter is analyzed through graphs. It is observed that temperature increases with higher values of inclination parameter. Trapping phenomena is discussed graphically.

Nomenclature.

a	Half width of the channel
b	Amplitude of wave
α	Angle of inclination
λ	Wave length of the peristaltic wave
λ_1	Jeffrey parameter
Fr	Froude number
c	Wave speed
\bar{t}	Time
(\bar{X}, \bar{Y})	Stationary coordinates
(\bar{x}, \bar{y})	Moving coordinates



(\bar{U}, \bar{V})	Velocity components in fixed frame
(\bar{u}, \bar{v})	Velocity components in moving frame
ϕ	Amplitude ratio
P	Pressure
θ	Dimensionless temperature distribution
T	Dimensional temperature distribution
T_0	Reference temperature
T_1	Temperature at the plates
μ	Viscosity
ν	Kinematic viscosity
k_0	Thermal conductivity
ρ	Density
σ	Permeability parameter
Da	Darcy's number
Gr	local temperature Grashof number
Re	Reynolds number
Pr	Prandtl number
Ec	Eckert number
δ	Wave number
N	Perturbation parameter
g	Acceleration due to gravity
q	Volume flow rate in fixed frame
Q	Volume flow rate in wave frame
F	Dimensionless mean flow in fixed frame
Θ	Dimensionless mean flow in wave frame
Δp	Pressure rise

1. Introduction

In recent times, peristalsis is a current area of research due to its wide industrial and biological applications. In peristaltic pumping the flow is generated by a progressive wave of area contraction or expansion along the tube walls. Very significant application of peristalsis by nature is observed in the flow of physiological fluids or biofluids from one part of the living body to the other. For example, swallowing of food through the esophagus, the colonic transport in the large intestine, the passage of urine from the kidney to the urinary bladder through the ureter, the spermatid flows in the ducts of the male reproductive tract, the vasomotion of small blood vessels and movement of ovum in the fallopian tube etc.

In view of such industrial and physiological applications, the peristaltic flow has been studied in literature by various researchers for different fluids under different conditions. Several theoretical and experimental studies have been carried out to understand the mechanism of peristaltic transport. The present study deals with peristaltic transport of nanofluids in a vertical porous stratum. The flow through porous media has a number of practical applications in engineering and medicine like extraction of energy from geothermal regions, oil flow through porous rocks and drug penetration through human skin.

The first experimental work on peristaltic transport was done by Latham [1]. Shapiro et al. [2] presented a detailed analysis of peristaltic flow of Newtonian fluid along with experimental results. Some

investigations on peristaltic flow of different physiological fluids are reported in earlier studies. [3-13]. Rudraiah and Nagaraj [14] considered natural convection along with the influence of Darcy and viscous resistances. A model of two-dimensional asymmetric channel is made by Mishra and Rao [15] to understand the fluid mechanic effects of peristaltic pumping. Vajravelu et al. [16] analyzed peristaltic flow of Hershel–Bulkley fluid in channel and extended the study for tube with inclination [17].

Kothandapani and Srinivas [18] analyzed Non-linear peristaltic transport of a Newtonian fluid in an inclined asymmetric channel through a porous medium. Haroun [19] examined the peristaltic flow of a fourth grade fluid in an inclined asymmetric channel. Hayat et al. [20] extended the investigation of Haroun [19] by incorporating the effects of an inclined magnetic field. Vajravelu et al. [21] investigated the influence of heat transfer on peristaltic transport of a Jeffrey fluid in a vertical porous stratum.

Mehmood et al. [22] studied the influence of heat transfer on peristaltic flow in inclined asymmetric channel for fourth grade fluid along with partial slip. MHD convection flow of a couple stress fluid through a vertical porous stratum is examined by Sreenadh et al. [23]. Prasad et al. [24] studied temperature dependent properties on MHD mixed convection heat transfer in a vertical channel with temperature dependent transport. Further, free convection flow of a Jeffrey fluid through a vertical deformable porous stratum is discussed by Sreenadh et al. [25].

Motivated by the earlier studies, it is interesting to study the effects of heat transfer on peristaltic transport of Jeffrey fluid in an inclined porous stratum. In this study, quite a few interesting features of the flow in porous medium and heat transfer characteristics have been discussed.

2. Mathematical formulation

We consider the peristaltic motion of Jeffrey fluid in a two dimensional channel. An infinite sinusoidal wave train propagating with constant wave speed c along the channel walls generates the flow as shown in Fig. 1. The wall deformations are given by

$$\bar{Y} = H(x,t) = a + bc \cos\left(\frac{2\pi}{\lambda}(x - ct)\right) \quad (1)$$

$$\bar{Y} = -H(x,t) = -a - bc \cos\left(\frac{2\pi}{\lambda}(x - ct)\right) \quad (2)$$

where $2a$ is the width of the channel, b is amplitude of wave, \bar{t} is the time and λ is wavelength.

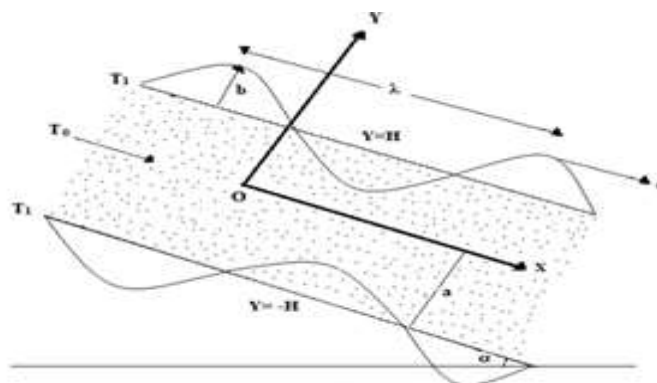


Figure 1. Physical Model

The constitutive equations for an incompressible Jeffrey fluid are

$$\bar{T} = -\bar{p}\bar{I} + \bar{s} \quad (3)$$

$$\bar{s} = \frac{\mu}{1 + \lambda_1} (\dot{\bar{\gamma}} + \lambda_2 \ddot{\bar{\gamma}}) \quad (4)$$

Where \bar{T} - Cauchy stress tensor, \bar{S} - Extra stress tensor, \bar{p} - pressure, \bar{I} - Identity tensor, λ_1 - ratio of relaxation time to retardation time, λ_2 - retardation time and $\dot{\bar{\gamma}}$ - shear rate.

Under the assumption that the length of the channel is an integral multiple of wavelength λ , the flow is unsteady in the stationary frame and it is assumed to be steady in the moving frame of reference. The transformation between stationary coordinates (\bar{X}, \bar{Y}) and moving coordinates (\bar{x}, \bar{y}) is given by

$$\bar{x} = \bar{X} - c\bar{t}, \quad \bar{y} = \bar{Y}, \quad \bar{u} = \bar{U} - c, \quad \bar{v} = \bar{V}, \quad \bar{p} = \bar{P}(x, t) \quad (5)$$

here \bar{U}, \bar{V} denotes the velocity components in fixed coordinates. \bar{u}, \bar{v} are the velocity components in moving coordinates respectively.

The non-dimensional quantities are,

$$\left. \begin{aligned} x &= \frac{2\pi\bar{x}}{\lambda}, \quad y = \frac{\bar{y}}{a}, \quad u = \frac{\bar{u}}{c}, \quad v = \frac{\bar{v}}{c\delta}, \quad \delta = \frac{2\pi a}{\lambda}, \quad p = \frac{2\pi a^2 \bar{p}}{\mu c \lambda}, \quad t = \frac{2\pi c \bar{t}}{\lambda}, \\ h &= \frac{H}{a}, \quad S = \frac{a}{\mu c} \bar{S}, \quad \phi = \frac{b}{a}, \quad \sigma = \frac{a}{\sqrt{k}}, \quad \nu = \frac{\mu}{\rho_0}, \quad T = \theta(T_1 - T_0) + T_0, \\ Gr &= \frac{\alpha g(T_1 - T_0)a^3}{\nu^2}, \quad Pr = \frac{\mu c_p}{k_0}, \quad Re = \frac{ac}{\nu}, \quad G = \frac{Gr}{Re}, \quad Ec = \frac{c^2}{c_p(T_1 - T_0)}, \\ N &= Ec Pr, \quad f = \frac{Re}{Fr}, \quad Fr = \frac{c^2}{ag} \end{aligned} \right\} \quad (6)$$

Where Re - Reynolds number, σ - permeability, Gr - Grashof number, Pr - Prandtl number, δ - wave number, Ec - Eckert number, Fr - Froude number and N - perturbation parameter.

The non-dimensional governing equations are,

$$\frac{\partial u}{\partial x} + \frac{\partial v}{\partial y} = 0 \quad (7)$$

$$\delta Re \left[(u+1) \frac{\partial u}{\partial x} + v \frac{\partial u}{\partial y} \right] = -\frac{\partial p}{\partial x} + \delta \frac{\partial S_{xx}}{\partial x} + \frac{\partial S_{xy}}{\partial y} - \sigma^2 (u+1) + G\theta + f \sin \alpha \quad (8)$$

$$\delta^3 Re \left[(u+1) \frac{\partial v}{\partial x} + v \frac{\partial v}{\partial y} \right] = -\frac{\partial p}{\partial y} + \delta^2 \frac{\partial S_{xy}}{\partial x} + \delta \frac{\partial S_{yy}}{\partial y} - \delta^2 \sigma^2 v - \delta f \cos \alpha \quad (9)$$

$$\delta Pr Re \left[(u+1) \frac{\partial \theta}{\partial x} + v \frac{\partial \theta}{\partial y} \right] = \left[\frac{\partial^2 \theta}{\partial x^2} \delta^2 + \frac{\partial^2 \theta}{\partial y^2} \right] + 2\delta^2 N \left[\left(\frac{\partial u}{\partial x} \right)^2 + \left(\frac{\partial v}{\partial y} \right)^2 \right] + N \left(\delta^2 \frac{\partial v}{\partial x} + \frac{\partial u}{\partial y} \right)^2 + N \sigma^2 (u+1)^2 \quad (10)$$

$$\text{where } S_{xx} = \frac{2\delta}{1 + \lambda_1} \left[1 + \frac{\delta \lambda_2 c}{a} \left(u \frac{\partial}{\partial x} + v \frac{\partial}{\partial y} \right) \right] \frac{\partial u}{\partial x}, \quad S_{xy} = \frac{1}{1 + \lambda_1} \left[1 + \frac{\delta \lambda_2 c}{a} \left(u \frac{\partial}{\partial x} + v \frac{\partial}{\partial y} \right) \right] \left(\frac{\partial u}{\partial y} + \delta \frac{\partial v}{\partial x} \right)$$

$$S_{yy} = \frac{-2\delta}{1+\lambda_1} \left[1 + \frac{\delta\lambda_2 c}{a} \left(u \frac{\partial}{\partial x} + \frac{v}{\delta} \frac{\partial}{\partial y} \right) \right] \frac{\partial u}{\partial y}$$

$$\text{and } \left(\frac{\partial S_{xy}}{\partial y} \right)_{\delta \rightarrow 0} = \frac{1}{1+\lambda_1} \frac{\partial^2 u}{\partial y^2}$$

The corresponding boundary conditions are

$$\left. \begin{aligned} u = -1, \theta = 1 \quad \text{at } y = h(x) \\ \frac{\partial u}{\partial y} = 0, \frac{\partial \theta}{\partial y} = 0 \quad \text{at } y = 0 \end{aligned} \right\} \quad (11)$$

using long wavelength approximations and neglecting the wave number δ , equations (8)-(11) reduces to

$$-\frac{\partial p}{\partial x} + \frac{1}{1+\lambda_1} \frac{\partial^2 u}{\partial y^2} - \sigma^2 (u+1) + G\theta + f \sin \alpha = 0 \quad (12)$$

$$\frac{\partial p}{\partial y} = 0 \quad (13)$$

$$\frac{\partial^2 \theta}{\partial y^2} + N \left(\frac{\partial u}{\partial y} \right)^2 + N\sigma^2 (u+1)^2 = 0 \quad (14)$$

$$\left. \begin{aligned} u = -1, \theta = 1 \quad \text{at } y = h(x) \\ \frac{\partial u}{\partial y} = 0, \frac{\partial \theta}{\partial y} = 0 \quad \text{at } y = 0 \end{aligned} \right\} \quad (15)$$

The dimensional fluxes in the fixed and moving frames are

$$q = \int_0^{h(\bar{x})} \bar{u}(\bar{x}, \bar{y}) d\bar{y} \quad (16)$$

$$Q = \int_0^{H(\bar{x}, t)} \bar{U}(\bar{X}, \bar{Y}, \bar{t}) d\bar{Y} \quad (17)$$

From Eqs. (16) and (17) we have,

$$Q = q + c\bar{h}(\bar{x}) \quad (18)$$

The average time mean flow over a period T at a fixed position \bar{x} is

$$\bar{Q} = \frac{1}{T} \int_0^T Q dt = q + ac \quad (19)$$

The non-dimensional mean flow Θ in fixed frame and F in the wave frame are related as $\Theta = F + 1$

$$\text{where } F = \int_0^h u dy = \frac{q}{ac}, \quad \Theta = \frac{\bar{Q}}{ac}$$

3. Perturbation solution

To obtain the perturbation solution, the following quantities are expanded in powers of small parameter N as

$$\begin{aligned}
 u &= u_0 + Nu_1 + \dots \\
 \theta &= \theta_0 + N\theta_1 + \dots \\
 p &= p_0 + Np_1 + \dots
 \end{aligned}
 \tag{20}$$

Using the equation (20), equations (12) - (15) reduces to two different systems of equations.

Zero order system N^0 :

$$-\frac{dp_0}{dx} + \frac{1}{1+\lambda_1} \frac{\partial^2 u_0}{\partial y^2} - \sigma^2 (u_0 + 1) + G\theta_0 + f \sin \alpha = 0 \tag{21}$$

$$\frac{\partial^2 \theta_0}{\partial y^2} = 0 \tag{22}$$

The appropriate boundary conditions are

$$\left. \begin{aligned}
 u_0 &= -1 \text{ and } \theta_0 = 1 \text{ at } y = h \\
 \frac{\partial u_0}{\partial y} &= 0 \text{ and } \frac{\partial \theta_0}{\partial y} = 0 \text{ at } y = 0
 \end{aligned} \right\}
 \tag{23}$$

First order system N^1 :

$$-\frac{dp_1}{dx} + \frac{1}{1+\lambda_1} \frac{\partial^2 u_1}{\partial y^2} - \sigma^2 u_1 + G\theta_1 = 0 \tag{24}$$

$$\frac{\partial^2 \theta_1}{\partial y^2} + \left(\frac{\partial u_0}{\partial y} \right)^2 + \sigma^2 (u_0 + 1)^2 = 0 \tag{25}$$

The appropriate boundary conditions are

$$\left. \begin{aligned}
 u_1 &= 0 \text{ and } \theta_1 = 0 \text{ at } y = h \\
 \frac{\partial u_1}{\partial y} &= 0 \text{ and } \frac{\partial \theta_1}{\partial y} = 0 \text{ at } y = 0
 \end{aligned} \right\}
 \tag{26}$$

Solving equations (21) - (22) and (24) - (25) using boundary conditions (23) and (26), we get expressions for fluid velocity and temperature as

$$u_0 = \left(\frac{\frac{dp_0}{dx} - G - f \sin \alpha}{\sigma^2} \right) \frac{\cosh \sigma \sqrt{1+\lambda_1} y}{\cosh \sigma \sqrt{1+\lambda_1} h} - \left(\frac{\frac{dp_0}{dx} + \sigma^2 - G - f \sin \alpha}{\sigma^2} \right) \tag{27}$$

$$\theta_0 = 1 \tag{28}$$

$$\begin{aligned}
 u_1 &= \frac{dp_1}{dx} \left(\frac{\cosh \sigma \sqrt{1+\lambda_1} y}{\sigma^2 \cosh \sigma \sqrt{1+\lambda_1} h} - \frac{1}{\sigma^2} \right) + (GA_1(A_8 + A_9) - A_{10}) \left(\frac{\cosh \sigma \sqrt{1+\lambda_1} y}{\cosh \sigma \sqrt{1+\lambda_1} h} \right) \\
 &\quad - GA_1 \left(-\frac{A_2}{2\sigma^2} y^2 - \frac{A_3}{3\sigma^2} \cosh 2\sigma \sqrt{1+\lambda_1} y + \frac{A_4}{2\sigma} y \sinh \sigma \sqrt{1+\lambda_1} y \right) + A_{10}
 \end{aligned}
 \tag{29}$$

$$\theta_1 = A_1 \left(A_2 \frac{y^2}{2} - A_3 \cosh 2\sigma \sqrt{1+\lambda_1} y + A_4 \cosh \sigma \sqrt{1+\lambda_1} y \right) + A_{15} \tag{30}$$

The zeroth-order and first-order dimension less mean flow are given by

$$F_0 = \frac{dp_0}{dx} \left(\frac{\sinh \sigma \sqrt{1+\lambda_1} h}{\sigma^3 \sqrt{1+\lambda_1} \cosh \sigma \sqrt{1+\lambda_1} h} - \frac{h}{\sigma^2} \right) - (G + f \sin \alpha) \left(\frac{\sinh \sigma \sqrt{1+\lambda_1} h}{\sigma^3 \sqrt{1+\lambda_1} \cosh \sigma \sqrt{1+\lambda_1} h} - \frac{h}{\sigma^2} \right) - h \quad (31)$$

$$F_1 = \frac{dp_1}{dx} A_{11} + A_{12} - GA_1 (A_{13} + A_{14}) + A_{10} h \quad (32)$$

Solving equations (31) and (32) for $\frac{dp_0}{dx}$ and $\frac{dp_1}{dx}$ respectively yields,

$$\begin{aligned} \frac{dp_0}{dx} &= \frac{F_0 + h + (G + f \sin \alpha) \left(\frac{\sinh \sigma \sqrt{1+\lambda_1} h}{\sigma^3 \sqrt{1+\lambda_1} \cosh \sigma \sqrt{1+\lambda_1} h} - \frac{h}{\sigma^2} \right)}{\left(\frac{\sinh \sigma \sqrt{1+\lambda_1} h}{\sigma^3 \sqrt{1+\lambda_1} \cosh \sigma \sqrt{1+\lambda_1} h} - \frac{h}{\sigma^2} \right)} \\ &= \frac{\theta_0 - 1 + h + (G + f \sin \alpha) \left(\frac{\sinh \sigma \sqrt{1+\lambda_1} h}{\sigma^3 \sqrt{1+\lambda_1} \cosh \sigma \sqrt{1+\lambda_1} h} - \frac{h}{\sigma^2} \right)}{\left(\frac{\sinh \sigma \sqrt{1+\lambda_1} h}{\sigma^3 \sqrt{1+\lambda_1} \cosh \sigma \sqrt{1+\lambda_1} h} - \frac{h}{\sigma^2} \right)} \end{aligned} \quad (33)$$

$$\frac{dp_1}{dx} = \frac{F_1 - A_{12} + GA_1 (A_{13} + A_{14}) - A_{10} h}{A_{11}} = \frac{\theta_1 - A_{12} + GA_1 (A_{13} + A_{14}) - A_{10} h}{A_{11}} \quad (34)$$

The pressure rise for zeroth order and first order are expressed as,

$$\Delta p_0 = \int_0^1 \frac{dp_0}{dx} dx \quad \text{and} \quad \Delta p_1 = \int_0^1 \frac{dp_1}{dx} dx \quad (35)$$

4. Results and Discussion

The peristaltic pumping of Jeffrey fluid in an inclined porous stratum along with the effect of heat transfer are studied in the present problem. The effects of various pertinent parameters like Jeffrey parameter λ_1 , permeability parameter σ , angle of inclination α and perturbation parameter N on velocity, temperature and pressure rise are analyzed through graphs. The velocity profiles for different values of λ_1 , σ , α and N are plotted in Figs. 2 to 5 respectively. From Fig.2 it is observed that velocity increase with increasing values of Jeffrey parameter λ_1 . The variation in velocity profiles for different values of permeability parameter is depicted in Fig.3. It is clear that velocity reduces as permeability σ increases. The influence of angle of inclination on fluid velocity profiles are observed from Fig.4. It is found that the fluid velocity enhances with inclination parameter α . Fig. 5 shows that velocity increases with increasing values of perturbation parameter N .

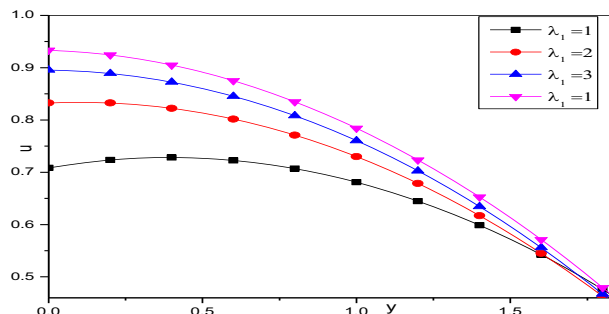


Figure 2. Velocity profiles for different values of λ_1 with $\phi = 0.6, f = 0.1, Gr = 0.1, Re = 0.1, N = 0.1, \sigma = 1, \alpha = \pi / 4$

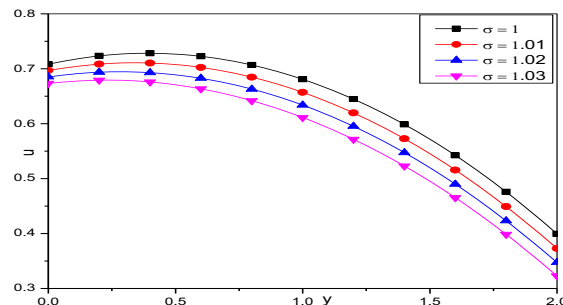


Figure 3. Velocity profiles for different values of σ with $\phi = 0.6, f = 0.1, Gr = 0.1, Re = 0.1, N = 0.1, \lambda_1 = 1, \alpha = \pi / 4$

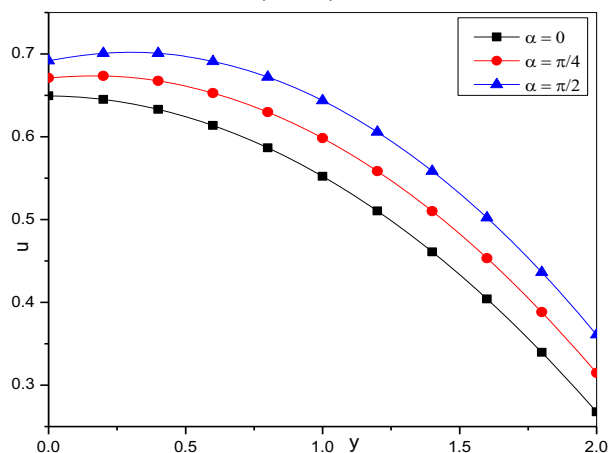


Figure 4. Velocity profiles for different values of α with $\phi = 0.6, f = 0.1, Gr = 0.1, Re = 0.1, N = 0.1, \sigma = 1, \lambda_1 = 1$

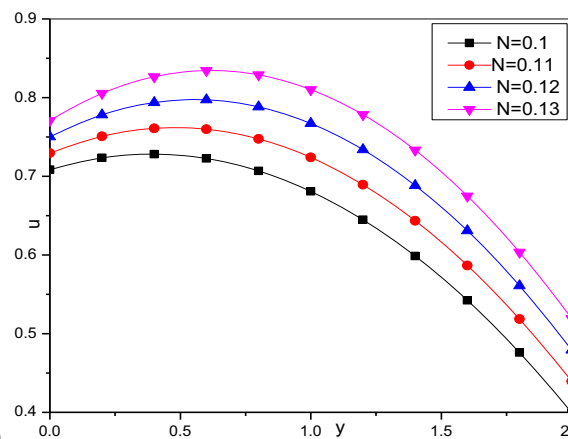


Figure 5. Velocity profiles for different values of N with $\phi = 0.6, f = 0.1, Gr = 0.1, Re = 0.1, \sigma = 1, \lambda_1 = 1, \alpha = \pi / 4$

The variation of temperature for different physical parameters $\lambda_1, \sigma, \alpha$ and N are presented from Figs. 6 to 9. The temperature increases with growing values of Jeffrey parameter λ_1 is illustrated in Fig.6. The effect of permeability parameter on temperature variation is noticed from Fig. 7 and temperature decreases with higher values of σ . The variation in temperature with different values of inclination parameter is illustrated in Fig. 8 and it is clear that temperature increases with increasing values of α . The influence of perturbation parameter on temperature is shown in Fig.9. It is noticed that temperature increases with rising values of N .

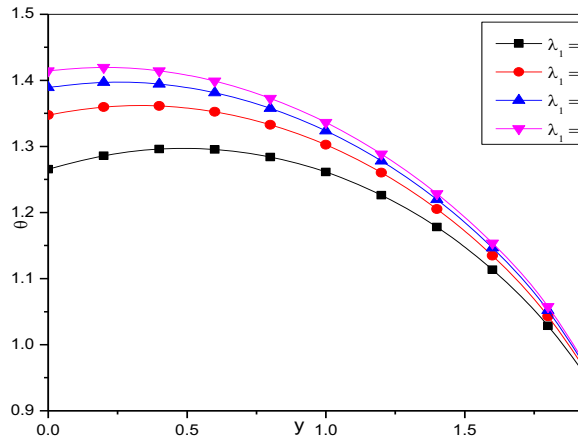


Figure 6. Temperature profiles for different values of λ_1 with $\phi = 0.6, f = 0.1, Gr = 0.1, Re = 0.1, N = 0.1, \sigma = 1, \alpha = \pi / 4$

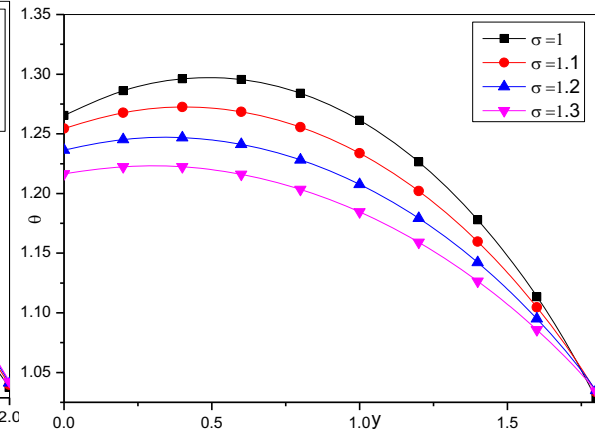


Figure 7. Temperature profiles for different values of σ with $\phi = 0.6, f = 0.1, Gr = 0.1, Re = 0.1, N = 0.1, \lambda_1 = 1, \alpha = \pi / 4$

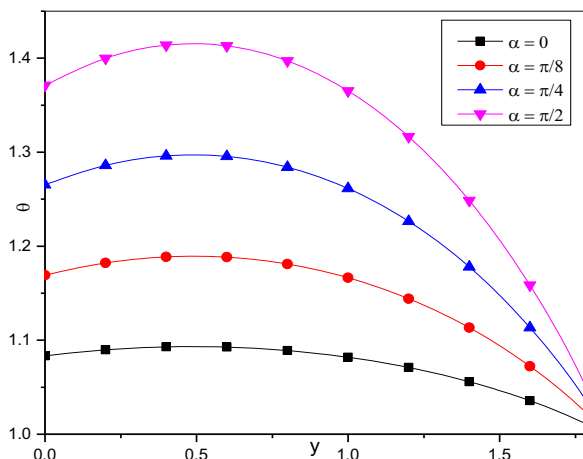


Figure 8. Temperature profiles for different values of α with $\phi = 0.6, f = 0.1, Gr = 0.1, Re = 0.1, N = 0.1, \sigma = 1, \lambda_1 = 1$

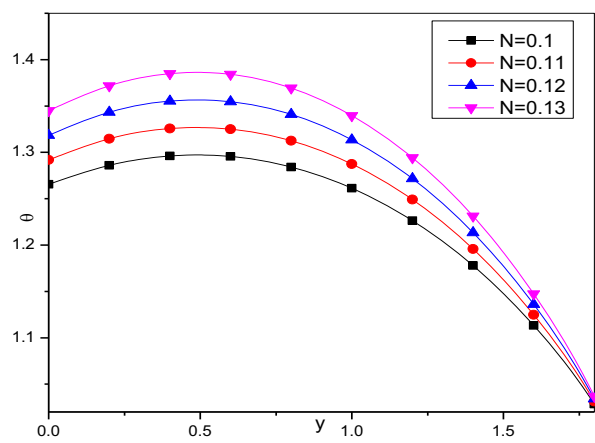


Figure 9. Temperature profiles for different values of N with $\phi = 0.6, f = 0.1, Gr = 0.1, Re = 0.1, \sigma = 1, \lambda_1 = 1, \alpha = \pi / 4$

The variation in pressure rise per wavelength with the mean flow for different values of $\lambda_1, \sigma, \alpha$ and N are given in Figs. 10 to 13. It is observed that the pressure rise over one period decreases with increasing mean flow. From Fig. 10 it is found that for fixed mean flow the pressure rise decreases with increasing values of Jeffrey parameter λ_1 . The effect of permeability parameter σ on variation of pressure rise along with mean flow is presented in Fig. 11. It is clear that the pressure rise decreases with increasing values of σ for fixed mean flow. The pressure rise with mean flow for different values of α and N are shown in Figs. 12 and 13 respectively. It is noticed that pressure rise increases as inclination parameter and perturbation parameter increases.

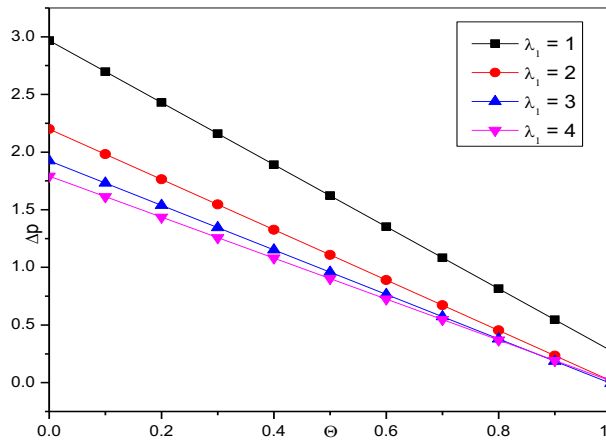


Figure 10. Pressure rise vs. mean flow different values of λ_1 with $\phi = 0.6, f = 0.1, Gr = 0.1, Re = 0.1, N = 0.1, \sigma = 1, \alpha = \pi / 4$

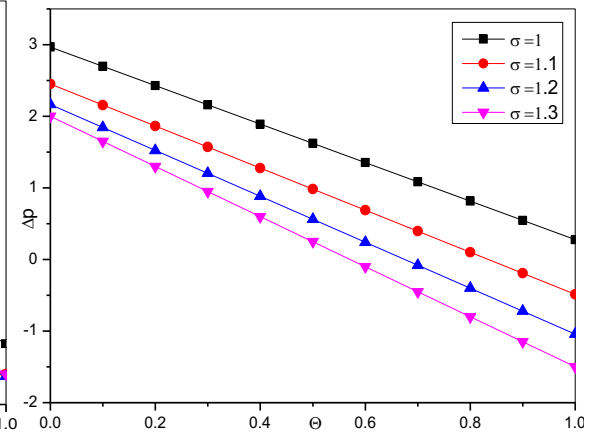


Figure 11. Pressure rise vs. mean flow for different values of σ $\phi = 0.6, f = 0.1, Gr = 0.1, Re = 0.1, N = 0.1, \lambda_1 = 1, \alpha = \pi / 4$

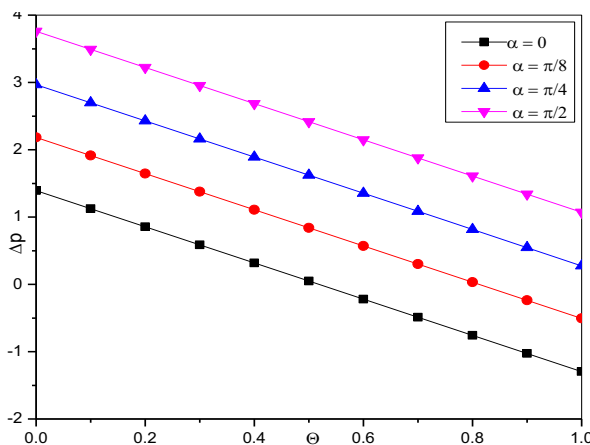


Figure 12. Pressure rise vs. mean flow for different values of α with $\phi = 0.6, f = 0.1, Gr = 0.1, Re = 0.1, N = 0.1, \sigma = 1, \lambda_1 = 1$

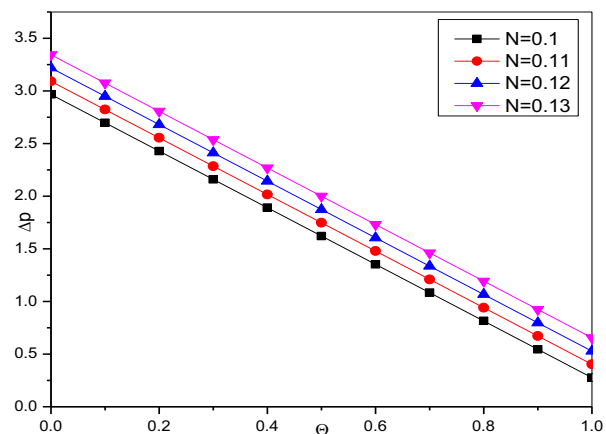


Figure 13. Pressure rise vs. mean flow for different values of N with $\phi = 0.6, f = 0.1, Gr = 0.1, Re = 0.1, \sigma = 1, \lambda_1 = 1, \alpha = \pi / 4$

The pressure gradient for various values of $\lambda_1, \sigma, \alpha$ and N are given in Figs. 14 to 17. It is noticed that the pressure gradient increases with increasing values of Jeffrey parameter λ_1 and permeability parameter σ . Also the pressure gradient reduces with higher values of inclination parameter α and perturbation parameter N . Further it is seen that the maximum pressure gradient occurs at $x = 0.75$.

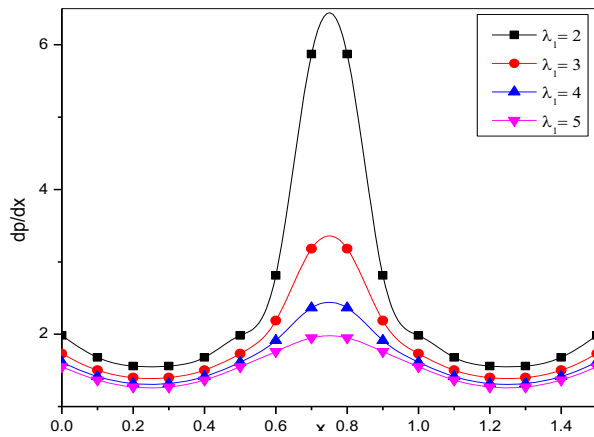


Figure 14. Pressure gradient vs. x for different values of λ_1 with $\phi = 0.6, f = 0.1, Gr = 0.1, Re = 0.1, N = 0.1, \sigma = 1, \alpha = \pi / 4$

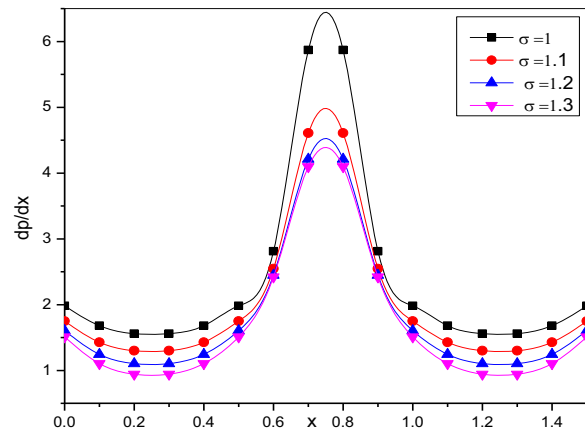


Figure 15. Pressure gradient vs. x for different values of σ with $\phi = 0.6, f = 0.1, Gr = 0.1, Re = 0.1, N = 0.1, \lambda_1 = 1, \alpha = \pi / 4$

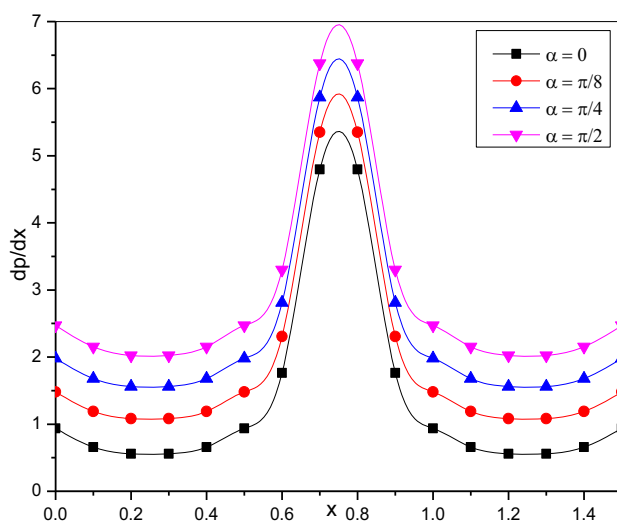


Figure 16. Pressure gradient vs. x for different values of α with $\phi = 0.6, f = 0.1, Gr = 0.1, Re = 0.1, N = 0.1, \sigma = 1, \lambda_1 = 1$

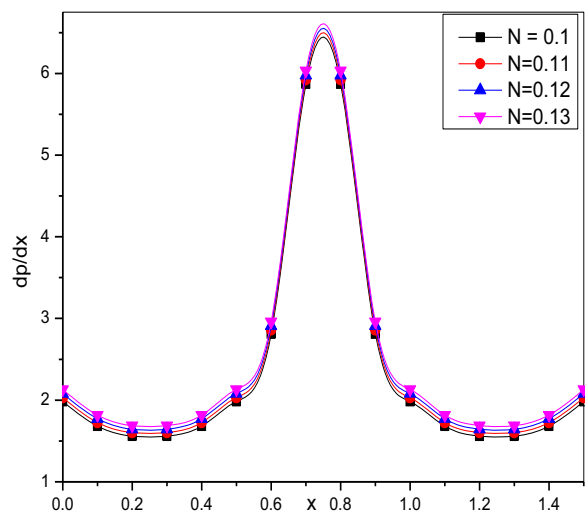


Figure 17. Pressure gradient vs. x for different values of N with $\phi = 0.6, f = 0.1, Gr = 0.1, Re = 0.1, \sigma = 1, \lambda_1 = 1, \alpha = \pi / 4$

5. Trapping Phenomena:

The other interesting phenomenon of peristalsis is trapping, the formation of internally circulating bolus of fluid which moves along with the wave. The effects of different pertinent parameters on the size of trapped bolus are presented in Figs. 18-21. It is found that the size of tapered bolus increases with increasing values of Jeffrey parameter λ_1 , Permeability parameter σ and inclination parameter α . Also, it is noticed that the size of bolus decreases with increasing values of perturbation parameter N .

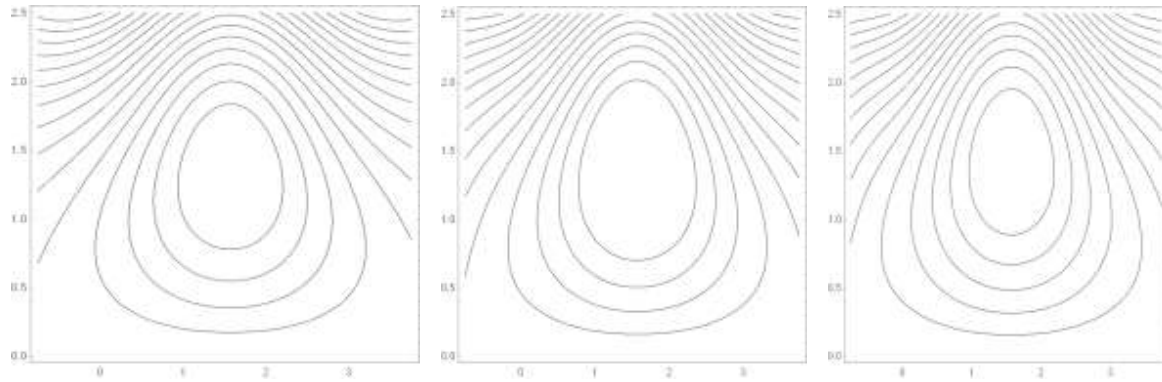


Figure 18. Streamlines with $\phi = 0.6, f = 0.1, Gr = 0.1, Re = 0.1, N = 0.1, \sigma = 1, \alpha = \pi / 4$ for different values of
i) $\lambda_1 = 1.5$, *ii)* $\lambda_1 = 2.5$, *iii)* $\lambda_1 = 3.5$

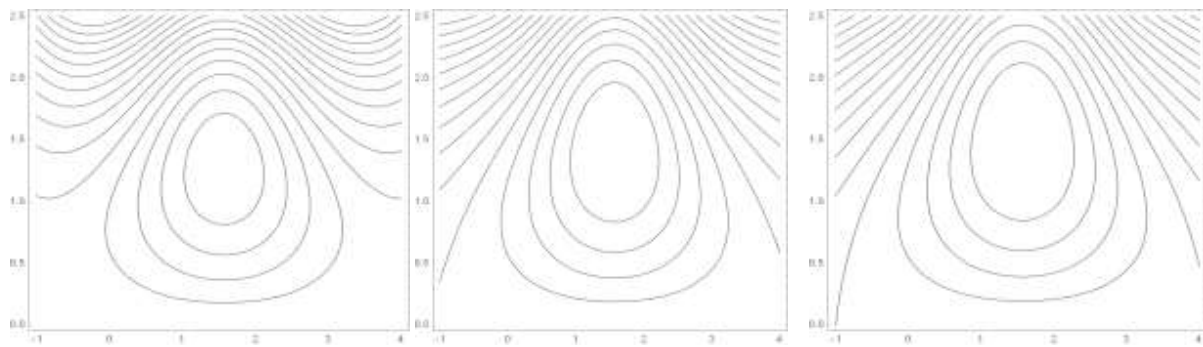


Figure 19. Streamlines with $\phi = 0.6, f = 0.1, Gr = 0.1, Re = 0.1, N = 0.1, \lambda_1 = 1, \alpha = \pi / 4$ for different values of
i) $\sigma = 1$, *ii)* $\sigma = 1.2$ *iii)* $\sigma = 1.4$

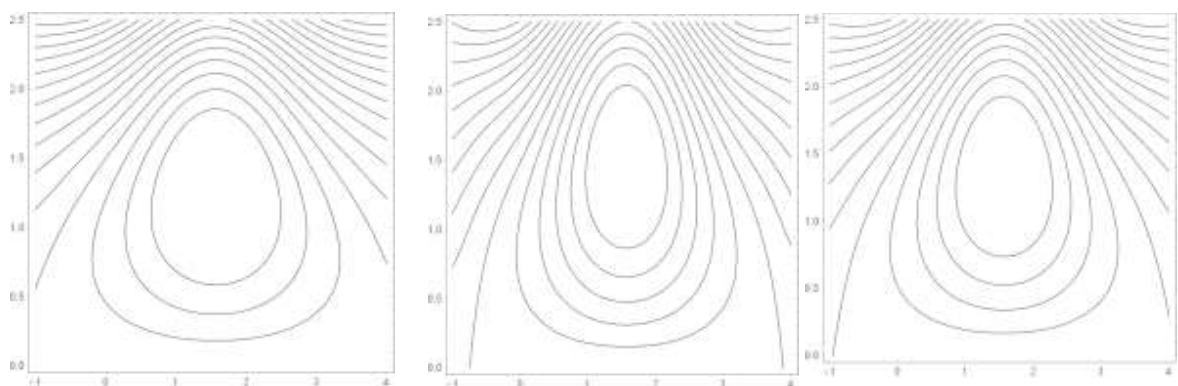


Figure 20. Streamlines with $\phi = 0.6, f = 0.1, Gr = 0.1, Re = 0.1, N = 0.1, \lambda_1 = 1, \sigma = 1$ for different values of
i) $\alpha = 0$, *ii)* $\alpha = \pi / 4$ *iii)* $\alpha = \pi / 2$

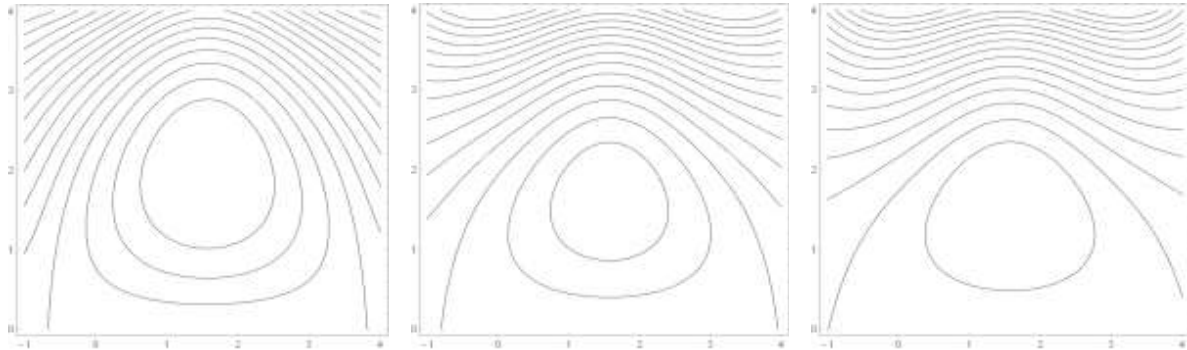


Figure 21. Streamlines with $\phi = 0.6, f = 0.1, Gr = 0.1, Re = 0.1, \alpha = \pi/4, \lambda_1 = 1, \sigma = 1$ for different values of N *i) N = 0.01, ii) N = 0.02 iii) N = 0.03*

6. Conclusions

The effect of heat transfer on peristaltic flow of Jeffrey fluid in an inclined porous stratum is studied in the present problem. The perturbation technique is used to solve the governing equations. The analytic solution for velocity, temperature and pressure gradient are derived. The effect of different physical parameters on flow characteristics are analyzed graphically. The significant observations are summarized as

1. The velocity in an inclined porous stratum enhances with greater values of Jeffrey parameter λ_1 , inclination parameter α and perturbation parameter N where the opposite behavior is observed with growing values of permeability σ .
2. The temperature in an inclined porous stratum increases with increasing values of λ_1 , α and N where as higher values of σ reduces the temperature profile.
3. For fixed mean flow the pressure rise increases as inclination parameter α and perturbation parameter N increases. Also the decrease in pressure rise noticed for increasing values of λ_1 and σ .
4. The pressure gradient enhances with higher values of λ_1 and σ where as it decreases with increasing values of α and N . The maximum pressure gradient occurs at $x = 0.75$
5. The size of the tapered bolus increases with increasing values of λ_1 , σ and α where as bolus size decreases as N increases.

Appendix

$$A_1 = \frac{\left(\frac{dp_0}{dx} - G - f \sin \alpha\right)^2}{\sigma^2}, \quad A_2 = \frac{\lambda_1}{2 \cosh^2 \sigma \sqrt{1 + \lambda_1} h} - 1,$$

$$A_3 = \frac{2 + \lambda_1}{8\sigma^2(1 + \lambda_1) \cosh^2 \sigma \sqrt{1 + \lambda_1} h}, \quad A_4 = \frac{2}{\sigma^2(1 + \lambda_1) \cosh \sigma \sqrt{1 + \lambda_1} h}$$

$$A_5 = A_3 \cosh 2\sigma \sqrt{1 + \lambda_1} h, \quad A_6 = A_2 \frac{h^2}{2}, \quad A_7 = \frac{2}{\sigma^2(1 + \lambda_1)},$$

$$A_8 = -\frac{A_2}{2\sigma^2}h^2 - \frac{A_3}{3\sigma^2}\cosh 2\sigma\sqrt{1+\lambda_1}h, \quad A_9 = \frac{A_4}{2\sigma}h\sinh \sigma\sqrt{1+\lambda_1}h,$$

$$A_{10} = \frac{G}{\sigma^2}\left(\frac{A_1A_2}{\sigma^2(1+\lambda_1)} + A_{15}\right), \quad A_{11} = \frac{\sinh \sigma\sqrt{1+\lambda_1}h}{\sigma^3\sqrt{1+\lambda_1}\cosh \sigma\sqrt{1+\lambda_1}h} - \frac{h}{\sigma^2},$$

$$A_{12} = \left(\frac{GA_1(A_8 + A_9) - A_{10}}{\cosh \sigma\sqrt{1+\lambda_1}h}\right)\frac{\sinh \sigma\sqrt{1+\lambda_1}h}{\sigma\sqrt{1+\lambda_1}}, \quad A_{13} = -\frac{A_2}{6\sigma^2}h^3 - \frac{A_3\sinh 2\sigma\sqrt{1+\lambda_1}h}{6\sigma^3\sqrt{1+\lambda_1}},$$

$$A_{14} = \frac{A_4}{2\sigma}\left(\frac{h\cosh \sigma\sqrt{1+\lambda_1}h}{\sigma\sqrt{1+\lambda_1}} - \frac{\sinh \sigma\sqrt{1+\lambda_1}h}{\sigma^2(1+\lambda_1)}\right), \quad A_{15} = A_1(A_5 - A_6 - A_7).$$

References

- [1] Latham TW 1966 MS Thesis, M III Cambridge, Massachusetts Institute of Technology, Cambridge
- [2] Shapiro AH, Jaffrin MY and Weinberg SL 1969 *J. Fluid Mech.* **37** 799–825
- [3] Jaffrin MY and Shapiro AH 1971 *Ann. Rev. Fluid Mech.* **3** 13–35
- [4] Burns JC and Parkes J 1967 *J. Fluid Mech.* **29** 731–743
- [5] Barton C and Raymor S 1968 *Bull. Math. Bio. Phy.* **30** 663–680
- [6] Chow TS 1970 *J. Appl. Mech.* **37** 901–906.
- [7] Jaffrin MY 1973 *Int. J. Eng. Sci.* **11** 681–699
- [8] Liron N 1976 *Bull. Math. Biol.* **38** pp 573–596
- [9] Takabatake S and Ayukawa K 1982 *J. Fluid Mech.* **122** 439–465
- [10] Radhakrishnamacharya G 1982 *Rheol. Acta.* **21** 30–35
- [11] Raju KK and Devanathan R 1972 *Rheol. Acta* **11** 170–178
- [12] Raju KK and Devanathan R 1974 *Rheol. Acta* **13** 944–948
- [13] Srivastava LM 1986 *Rheol. Acta.* **25** 638–641.
- [14] Rudraiah N and Nagaraj ST 1977 *Int. J. Engg. Sci.* **15** 589-600
- [15] Mishra M and Ramachandra Rao A 2003 *ZAMP* **54** 532–550.
- [16] Vajravelu K, Sreenadh S and Ramesh Babu V 2005 *Int. J. Non linear Mech.* **40** 83-90
- [17] Vajravelu K, Sreenadh S and Ramesh babu, V 2005 *Appl. Math. Computation.* **169** 726-735
- [18] Kothandapani M, and Srinivas S 2008 *Physics Letters A.* **372** 1265–1276
- [19] Haroun MH 2007 *Computational Materials Science.* **39** 324–333
- [20] Hayat T, Asghar Z, Asghar S and Mesloub S *J. the Taiwan Inst. Chem. Eng.* **41** 553–563
- [21] Vajravelu K, Sreenadh S and Lakshminarayana P 2011 *Commun. Nonlinear Sci. Numer. Simul.* **16** 3107–3125
- [22] Mehmood OU, Mustapha N and Shafie S 2012 *App. Math. and Mech.* **33** 1313– 1328
- [23] Sreenadh S, Sudhakara E, Krishnamurthy M and Gopi Krishna G 2015 *World App. Sci. J.* **33** 918-930
- [24] Prasad KV, Vaidya HM and Vajravelu K 2015 *J. App. Fluid Mech.* **8** 693-701

- [25] Sreenadh S, Rashidi MM, Kumara swamy Naidu K and Parandhama A 2016 *J. App. Mech.* **9** 2391-2401